TIT/HEP-405/NP

Finite Quark Mass Effects in the Improved Ladder Bethe–Salpeter Amplitudes

K. Naito[1], K. Yoshida, Y. Nemoto, M. Oka

Department of Physics, Tokyo Institute of Technology,

Meguro, Tokyo 152-8551, Japan

M. Takizawa[2]

Laboratory of Computer Sciences, Showa College of Pharmaceutical Sciences,

Machida, Tokyo 194-8543, Japan

Abstract

We study the finite quark mass effects of the low-energy QCD using the improved ladder Schwinger–Dyson and Bethe–Salpeter equations which are derived in the manner consistent with the vector and axial-vector Ward–Takahashi identities. The non-perturbative mass-independent renormalization allows us to calculate the quark condensate for a non-zero quark mass. We explicitly show that the PCAC relation holds. The key ingredients are the Cornwall–Jackiw–Tomboulis effective action, the generalized Noether current and the introduction of the regularization function to the Lagrangian. The reasonable values of the pion mass, the pion decay constant and the quark condensate are obtained with a rather large $\Lambda_{\rm QCD}$. The pion mass square and the pion decay constant are almost proportional to the current quark mass up to the strange quark mass region. It suggests that the chiral perturbation is applicable up to the strange quark mass region. We study the validity of the approximation often used in solving the Bethe–Salpeter equations too.

[1]E-mail address: kenichi@th.phys.titech.ac.jp

[2]E-mail address: takizawa@ac.shoyaku.ac.jp

1 Introduction

The program to derive the observed properties of hadrons non-perturbatively in QCD has been pursued with great intensity but not accomplished yet. The concept of chiral symmetry and its spontaneous breakdown are among the most important aspects of low-energy hadron physics. The spontaneous breakdown of chiral symmetry is believed to be responsible for a large part of the low-lying hadron masses as well as for the emergence of octet pseudoscalar mesons as Goldstone bosons. In order to explain the observed hadron spectrum, one also needs small, explicitly chiral-symmetry breaking terms, namely, the flavor-dependent current quark mass terms.

The Conwall–Jackiw–Tomboulis (CJT) effective action approach [1] for composite operators is widely used to study the dynamical symmetry breaking phenomena in the quantum field theories. The extremum condition for the effective action with respect to the quark propagator leads to the Schwinger–Dyson (SD) equation for the quark propagator on the non-perturbative vacuum and the second variational derivative of the effective action with respect to the quark propagator leads to the Bethe–Salpeter (BS) equation describing the bound states. The advantage of the present approach is that the derived SD and BS equations are consistent with the symmetry of the effective action evaluated in a certain approximation scheme.

The QCD SD equation for the quark propagator has been studied in the improved ladder approximation (ILA) by Higashijima [2] and Miransky [3]. They took the ladder diagrams of one-gluon exchange between q and $\bar{q}$ and assumed that the coupling constant is modified according to the standard perturbative corrections. It has been shown that the asymptotic behavior of the solution is consistent with the leading order renormalization group analysis while the infrared gluon exchange breaks chiral symmetry dynamically. Aoki et al. solved the BS equation the $J^{PC} = 0^{-+}\, q\bar{q}$ state and confirmed the existence of the Nambu–Goldstone pion in this approximation [4]. The numerical predictions of the pion decay constant f_π and the quark condensate $\langle\overline{\psi}\psi\rangle$ are rather good. It was also shown that the BS amplitude shows the correct asymptotic behavior as predicted by the OPE in QCD [5]. The masses and decay constants for the lowest lying scalar, vector and axial-vector mesons have been evaluated by calculating the two point correlation functions for the composite operators $\overline{\psi}M\psi$. The obtained

values are in good agreement with the observed ones [6].

So far, the current quark mass term has not been introduced in the studies of the BS amplitudes in the ILA. The purpose of the present paper is to investigate the effects of the finite current quark masses on the BS amplitudes for the $J^{PC} = 0^{-+}$ states. As shown in [2], the asymptotic behavior of the solution of the SD equation for the quark propagator with the finite current quark mass is rather different from that in the chiral limit. Therefore, it is important to study the effects of the finite current quark masses not only on the SD equations but also on the BS amplitudes.

There have been many studies of the pion BS amplitude using the effective models of QCD and/or the approximation schemes of the QCD [7, 8]. The advantages of the ILA model are as follows. (i) The model is given in the Lagrangian form so that one is able to apply the CJT effective action formulation and study symmetry properties of the system. (ii) The asymptotic behavior of the solutions of the SD and BS equations is consistent with the renormalization group analysis of QCD. (iii) It has been shown that the ILA model corresponds to the local potential approximation with the ladder part in the non-perturbative renormalization group approach [9]. (iv) The angular integration in the SD equation can be performed analytically. On the other hand, the disadvantages of the ILA model are as follows. (i) The axial-vector Ward–Takahashi identity is violated [10]. (ii) The quark may not be confined in the color singlet state.

In the finite quark mass case, it has been known that there is a difficulty in defining the quark condensate in the studies of the QCD SD equation. The extraction of the perturbative quark mass contribution in the UV region is not sufficient to remove the UV divergence in the SD equation since the SD equation includes the non-perturbative contribution even in the UV region. Inspired by Kusaka's idea of the non-perturbative renormalization of the fermion mass term in the mass-independent renormalization scheme [11], we propose a novel way to renormalize the SD equation and define the quark condensate with the finite quark mass.

The paper is organized as follows. In Sec. 2 we explain the ILA model Lagrangian we have used in the present study. In Sec. 3 the SD equation is derived from the CJT action and the renormalization of the SD equation is discussed in Sec. 4. In Sec. 5 our method of solving the BS equation for the pseudoscalar meson is presented. In Sec. 6 the formulation for the

meson decay constant is given and the low-energy theorem is discussed. Sec. 7 is devoted to the numerical results. Finally, summary and concluding remarks are given in Sec. 8.

2 Improved Ladder Model of QCD

We work with the following Lagrangian density of the improved ladder approximation(ILA) model of QCD proposed by Aoki et al. [4, 6],

$$\mathcal{L}[\psi,\overline{\psi}] := \mathcal{L}_{\rm free}[\psi,\overline{\psi}] + \mathcal{L}_{\rm int}[\psi,\overline{\psi}]\,, \tag{1}$$

$$\mathcal{L}_{\rm free}[\psi,\overline{\psi}] := \overline{\psi} f(\partial^2)(i\partial\!\!\!/ - m_0)\psi\,. \tag{2}$$

Here the function $f(\zeta)$ of $\zeta = \partial^2$ is introduced to provide a cut-off regularization of the ultraviolet divergences of the quark loops. The reason we introduce the cut-off function at the Lagrangian level is to preserve the consistency between the SD and BS equations. If one uses the regularization that is inconsistent between the SD and BS equations, the low-energy relation based on the chiral symmetry should be violated by the regularization. The function $f(\zeta)$ should satisfy $f(\zeta=0)=1$ and $f(\zeta)\to\infty$ for $\zeta \gg \Lambda_{\rm UV}^2$. In this paper, we employ the sharp cut-off function

$$f(\zeta) = 1 + M\theta(\zeta - \Lambda_{\rm UV}^2), \quad M\to\infty. \tag{3}$$

We introduce the bare mass of quarks m_0 which is evaluated at $\Lambda_{\rm UV}$.[4, 12] In general m_0 is a diagonal flavor matrix i.e. $m_0 = {\rm diag}(m_u, m_d, m_s)$ for $N_f = 3$. In this paper we deal only with a flavor independent mass and therefore the case with $SU(3)_F$ symmetry.

The interaction term is given by

$$\begin{aligned}\mathcal{L}_{\rm int}[\psi,\overline{\psi}](x) := & -\frac{1}{2}\int_{pp'qq'} \mathcal{K}^{mm',nn'}(p,p';q,q') \\ & \times \overline{\psi}_m(p)\psi_{m'}(p')\overline{\psi}_n(q)\psi_{n'}(q')e^{-i(p+p'+q+q')x}\,,\end{aligned} \tag{4}$$

$$\begin{aligned}\mathcal{K}^{mm',nn'}(p,p';q,q') = & \ \bar{g}^2\left((\frac{p_E-q'_E}{2})^2,(\frac{q_E-p'_E}{2})^2\right) \\ & \times iD^{\mu\nu}\left(\frac{p+p'}{2}-\frac{q+q'}{2}\right)(\gamma_\mu T^a)^{mm'}(\gamma_\nu T^a)^{nn'}\end{aligned} \tag{5}$$

where $\int_p$ denotes $\int\frac{d^4p}{(2\pi)^4}$ and p_E represents the Euclidean momentum. The Fourier transformations of fields are defined by $\overline{\psi}(p) = \int d^4x e^{ipx}\overline{\psi}(x)$ and $\psi(p) = \int d^4x e^{ipx}\psi(x)$. The indices

$m, n, \cdots$ are combined indices $m := (a, i, f)$, $n := (b, j, g), \cdots$ with Dirac indices $a, b, \cdots$ and color indices $i, j, \cdots$ and flavor indices $f, g, \cdots$. T^a denotes the generator of the color $SU(N_C)$. According to Higashijima and Miransky, we choose a particular set of the momenta that determines the running coupling constant, i.e.,

$$\bar{g}^2(p_E^2, q_E^2) = \theta(p_E^2 - q_E^2) g^2(p_E^2) + \theta(q_E^2 - p_E^2) g^2(q_E^2). \tag{6}$$

This way of introducing the running coupling constant is very natural from the non-perturbative renormalization group approach with the local potential approximation [9]. It is often called the Higashijima-Miransky approximation. The infrared cut-off $t_{\rm IF}$ is introduced in the running coupling constant as

$$g^2(p_E^2) := \begin{cases} \dfrac{1}{\beta_0} \dfrac{1}{1+t} & \text{for } t_{\rm IF} \le t \\ \dfrac{1}{2\beta_0} \dfrac{1}{(1+t_{\rm IF})^2} \left[3t_{\rm IF} - t_0 + 2 - \dfrac{(t-t_0)^2}{t_{\rm IF} - t_0} \right] & \text{for } t_0 \le t \le t_{\rm IF} \\ \dfrac{1}{2\beta_0} \dfrac{3t_{\rm IF} - t_0 + 2}{(1+t_{\rm IF})^2} & \text{for } t \le t_0 \end{cases} , \tag{7}$$

$$t := \ln \frac{p_E^2}{\Lambda_{\rm QCD}^2} - 1, \tag{8}$$

$$\beta_0 := \frac{1}{(4\pi)^2} \frac{11 N_C - 2 N_f}{3}. \tag{9}$$

Above $t_{\rm IF}$, $g^2(p_E^2)$ develops according to the one-loop result of the QCD renormalization group equation and below t_0, $g^2(p_E^2)$ is kept constant. These two regions are connected by the quadratic polynomial so that $g^2(p_E^2)$ becomes a smooth function. Here N_C is the number of colors and N_f is the number of active flavors. We use $N_C = N_f = 3$ in our numerical studies. The gluon propagator is given in the Landau gauge

$$iD^{\mu\nu}(k) = \left(g^{\mu\nu} - \frac{k^\mu k^\nu}{k^2} \right) \frac{-1}{k^2}. \tag{10}$$

3 SD equation

In order to derive the Schwinger–Dyson (SD) equation, we use the formalism of the Cornwall–Jackiw–Tomboulis (CJT) effective action [1] which is given by

$$\Gamma[S_F] := i\mathrm{TrLn}[S_F] - i\mathrm{Tr}[S_0^{-1}S_F] + \Gamma_{\mathrm{loop}}[S_F]. \tag{11}$$

The last term of Eq.(11) is the residual term. Multiplying a factor i, $i\Gamma_{\mathrm{loop}}[S_F]$ is given by the sum of all Feynman amplitudes of 2-loop or higher-loop 2-particle irreducible vacuum diagrams in which every bare quark propagator

$$S_0(x,y) = \int_q e^{-iq(x-y)} \frac{1}{f(-q^2)} \frac{i}{\not{q} - m_0} \tag{12}$$

is replaced by the full one

$$S_F(x,y) = \langle 0|T\psi(x)\overline{\psi}(y)|0\rangle. \tag{13}$$

The SD equation is the stability condition of the CJT action

$$\frac{\delta\Gamma[S_F]}{\delta S_{Fmn}(x,y)} = 0. \tag{14}$$

Throughout this paper, we employ the lowest order (lowest–loop) expansion of the $\Gamma_{\mathrm{loop}}[S_F]$ as

$$\begin{aligned} \Gamma_{\mathrm{loop}}[S_F] &= -\frac{1}{2}\int d^4x \mathcal{K}^{m_1m_2,n_1n_2}(i\partial_{x_1}, i\partial_{x_2}; i\partial_{y_1}, i\partial_{y_2}) \\ &\quad \times [S_{Fm_2m_1}(x_2,x_1)S_{Fn_2n_1}(y_2,y_1) - S_{Fm_2n_1}(x_2,y_1)S_{Fn_2m_1}(y_2,x_1)]\Big|_* \end{aligned} \tag{15}$$

where the symbol $*$ means to taking $x_1, x_2, y_1, y_2 \to x$ after all the derivatives are operated. This leads to the ILA model, where the SD equation is given in momentum space by

$$iS_F^{-1}(q) - iS_0^{-1}(q) + C_F \int_p \bar{g}^2(q_E^2, p_E^2) iD^{\mu\nu}(p-q)\gamma_\mu S_F(p)\gamma_\nu = 0\,, \tag{16}$$

with

$$C_F = \frac{\mathrm{tr}\,[T^aT^a]}{N_C} = \frac{N_C^2 - 1}{2N_C}\,. \tag{17}$$

Now we introduce the regularized propagator as

$$S_0^R(q) := f(-q^2)S_0(q) = \frac{i}{\not{q} - m_0}, \tag{18}$$

$$S_F^R(q) := f(-q^2)S_F(q). \tag{19}$$

Then the SD equation (16) becomes

$$iS_F^{R-1}(q) - iS_0^{R-1}(q) + \frac{C_F}{f(-q^2)}\int_p \frac{1}{f(-p^2)}\bar{g}^2(q_E^2,p_E^2)iD^{\mu\nu}(p-q)\gamma_\mu S_F^R(p)\gamma_\nu = 0 \tag{20}$$

in which one finds that the integral is cut-off at $p_E^2 = -p^2 = \Lambda_{\rm UV}^2$ due to the function $f(-p^2)$. Substituting the general form of the SD solution

$$S_F^R(q) = \frac{i}{A(q^2)\not{q} - B(q^2)} \tag{21}$$

we obtain a set of integral equations

$$\begin{aligned} A(q^2) &= 1 + \frac{iC_F}{q^2 f(-q^2)}\int_p \frac{\bar{g}^2(q_E^2,p_E^2)}{f(-p^2)}\frac{3(p^2+q^2)(pq) - 4(pq)^2 - 2p^2q^2}{(q-p)^4} \\ &\quad \times \frac{A(p^2)}{p^2A^2(p^2) - B^2(p^2)}, \end{aligned} \tag{22}$$

$$B(q^2) = m_0 + \frac{iC_F}{f(-q^2)}\int_p \frac{\bar{g}^2(q_E^2,p_E^2)}{f(-p^2)}\frac{1}{(p-q)^2}\frac{-3B(p^2)}{p^2A^2(p^2) - B^2(p^2)}. \tag{23}$$

After the Wick rotation, we obtain

$$A(-q_E^2) \equiv 1 \tag{24}$$

from Eq.(22). This is another advantage of the Higashijima–Miransky approximation, where the running coupling constant is defined so as to make the wave function renormalization Z_2 unity [4, 10]. Then we find an integral equation for $B(-q_E^2)$ as

$$B(-q_E^2) = m_0 + \frac{3C_F}{16\pi^2}\int_0^{\Lambda_{\rm UV}^2} dp_E^2\, \bar{g}^2(q_E^2,p_E^2)\frac{p_E^2}{\max\{q_E^2,p_E^2\}}\frac{B(-p_E^2)}{p_E^2 + B^2(-p_E^2)}. \tag{25}$$

4 Renormalization of quark mass

In this section we discuss the renormalization of the quark mass. The operator product expansion analysis shows that in the asymptotic region the QCD quark mass function $B(-q_E)$ for three quark flavors behaves as follows [13].

$$B(-q_E^2) = m_R(\mu^2)\left[\frac{g^2(q_E^2)}{g^2(\mu^2)}\right]^{4/9} - \xi_R(\mu^2)\frac{g^2(q_E^2)}{3q_E^2}\left[\frac{g^2(q_E^2)}{g^2(\mu^2)}\right]^{-4/9}, \tag{26}$$

where $m_R(\mu^2)$ is the current quark mass renormalized at μ^2 and $\xi_R(\mu^2) := \langle\overline{\psi}\psi\rangle_R$ is the quark condensate renormalized at μ^2. The improved ladder model of QCD is the model which is

constructed so as to reproduce the QCD asymptotic behavior. Therefore we introduce the renormalization condition of the quark mass so that the solution of the SD equation can be interpreted as the QCD quark mass function in the asymptotic region.

The quark mass function calculated in the effective model of QCD can be expressed in the similar fashion as Eq.(26)

$$B(-q_E^2) = m_R(\mu^2)\, F(q_E^2, \mu^2) - \xi_R(\mu^2)\, G(q_E^2, \mu^2)\,. \tag{27}$$

Then we introduce the renormalization condition

$$F(\mu^2, \mu^2) = 1\,, \tag{28}$$

which is equivalent to

$$\left.\frac{\partial B(-\mu^2)}{\partial m_R(\mu^2)}\right|_{m_R(\mu^2)=0} = 1\,. \tag{29}$$

This mass independent renormalization condition for the SD equation is first proposed by Kusaka [11]. The mass renormalization constant $Z_m = Z_m(\Lambda_{\rm UV}^2, \mu^2)$ is introduced by

$$m_0(\Lambda_{\rm UV}^2) = Z_m^{-1} m_R(\mu^2)\,. \tag{30}$$

It should be noted here that the renormalization constant is independent of mass in this renormalization scheme. It will be explicitly shown later in this section. By substituting m_0 by Eq.(30), the SD equation (25) becomes

$$B(-q_E^2) = Z_m^{-1}\, m_R(\mu^2) + \int_0^{\Lambda_{\rm UV}^2} dp_E^2\, K(q_E^2, p_E^2)\, \frac{B(-p_E^2)}{p_E^2 + B^2(-p_E^2)}\,, \tag{31}$$

with

$$K(q_E^2, p_E^2) := \frac{3C_F}{16\pi^2}\, \bar{g}^2(q_E^2, p_E^2) \frac{p_E^2}{\max\{q_E^2, p_E^2\}}\,. \tag{32}$$

By differentiating this equation with respect to $m_R(\mu^2)$ and taking $m_R(\mu^2) = 0$, one obtains

$$\begin{aligned}\left.\frac{\partial B(-q_E^2)}{\partial m_R(\mu^2)}\right|_{m_R(\mu^2)=0} &= Z_m^{-1} \\ &\quad + \int_0^{\Lambda_{\rm UV}^2} dp_E^2\, K(q_E^2, p_E^2)\, \frac{p_E^2 - B_0^2(-p_E^2)}{(p_E^2 + B_0^2(-p_E^2))^2}\, \left.\frac{\partial B(-p_E^2)}{\partial m_R(\mu^2)}\right|_{m_R(\mu^2)=0}\end{aligned} \tag{33}$$

The renormalization condition (29) leads to

$$Z_m^{-1} = 1 - \int_0^{\Lambda_{\rm UV}^2} dp_E^2\, K(\mu^2, p_E^2)\, \frac{p_E^2 - B_0^2(-p_E^2)}{\left(p_E^2 + B_0^2(-p_E^2)\right)^2}\, \left.\frac{\partial B(-p_E^2)}{\partial m_R(\mu^2)}\right|_{m_R(\mu^2)=0} . \tag{34}$$

Here $B_0(-q_E^2)$ is the solution of the SD equation in the chiral limit, namely,

$$B_0(-q_E^2) = \frac{3C_F}{16\pi^2} \int_0^{\Lambda_{\rm UV}^2} dp_E^2\, \bar{g}^2(q_E^2, p_E^2)\, \frac{p_E^2}{\max\{q_E^2, p_E^2\}}\, \frac{B_0(-p_E^2)}{p_E^2 + B_0^2(-p_E^2)} . \tag{35}$$

Now the combination of Eqs.(33) and (34) yields an integral equation for $\left.\frac{\partial B(-q_E^2)}{\partial m_R(\mu^2)}\right|_{m_R(\mu^2)=0}$. Eq.(34) explicitly shows that the mass renormalization constant Z_m does not depend on the quark mass.

In order to obtain the quark mass function with the renormalized current quark mass, one first calculates $B_0(-q_E^2)$ by solving the SD equation in the chiral limit Eq.(35). Next Z_m and $\left.\frac{\partial B(-q_E^2)}{\partial m_R(\mu^2)}\right|_{m_R(\mu^2)=0}$ are obtained by solving Eqs.(33) and Eq.(34). Finally Eq.(31) is solved to find $B(-q_E^2)$.

Let us now propose the following definition of the quark condensate.

$$\xi_R(\mu^2) := Z_m^{-1} \xi_0(\Lambda_{\rm UV}^2) , \tag{36}$$

$$\xi_0(\Lambda_{\rm UV}^2) := -\left(\int^{\Lambda_{\rm UV}} \frac{d^4q}{(2\pi)^4} {\rm tr}[S_F^R(q)] - \int^{\Lambda_{\rm UV}} \frac{d^4q}{(2\pi)^4} {\rm tr}[S_F^R(q)_{\rm pert}] \right) , \tag{37}$$

$$S_F^R(q) := \frac{i}{\not{q} - B(q^2)} , \tag{38}$$

$$S_F^R(q)_{\rm pert} := \left.\frac{\partial S_F^R(q)}{\partial m_R(\mu^2)}\right|_{m_R(\mu^2)=0} m_R(\mu^2) . \tag{39}$$

In order to avoid the divergence originated by the perturbative quark mass contribution to the quark condensate in the UV region, the perturbative quark mass contribution should be subtracted. The key point of our definition of the quark condensate is Eq.(39), namely, the perturbative quark mass contribution is defined using the fully calculated quark mass function $B(q^2)$. The subtraction of the perturbative quark mass contribution obtained by the operator product expansion approach in the UV region is not sufficient. Our definition of the quark condensate has the desirable property:

$$m_0(\Lambda_{\rm UV}^2)\, \xi_0(\Lambda_{\rm UV}^2) = m_R(\mu^2)\, \xi_R(\mu^2) . \tag{40}$$

5 BS equation for Pseudoscalar Mesons

The homogeneous BS equation is given by

$$\frac{\delta^2\Gamma[S_F]}{\delta S_{Fmn}(x,y)\delta S_{Fn'm'}(y',x')}\chi_{n'm'}(y',x';P_B)=0\,. \tag{41}$$

Here the BS amplitude is defined by

$$\chi_{nm}(y,x;P_B):=\langle 0|T\psi_n(y)\overline{\psi}_m(x)|\boldsymbol{P}_B\rangle \tag{42}$$

for a q-$\bar{q}$ state $|\boldsymbol{P}_B\rangle$. The normalization condition is $\langle \boldsymbol{P}_B|\boldsymbol{P}'_B\rangle=(2\pi)^3 2P_{B0}\delta^3(\boldsymbol{P}_B-\boldsymbol{P}'_B)$ and $P_B:=(\sqrt{M_B^2+\boldsymbol{P}_B^2},\boldsymbol{P}_B)$ is the on-shell momentum. Eq.(41) is expressed in momentum space

$$S_F^{-1}(q_+)\chi(q;P_B)S_F^{-1}(q_-)=-iC_F\int_k \bar{g}^2(q_E^2,k_E^2)iD^{\mu\nu}(q-k)\gamma_\mu\chi(k;P_B)\gamma_\nu\,, \tag{43}$$

with

$$q_+=q+\frac{P_B}{2},\quad q_-=q-\frac{P_B}{2}\,, \tag{44}$$

where the Fourier transformation of the BS amplitude is defined by

$$\chi_{nm}(y,x;P_B)=e^{-iP_BX}\int_q e^{-iq(y-x)}\chi_{nm}(q;P_B),\quad X=\frac{y+x}{2}. \tag{45}$$

We introduce the regularized BS amplitude by

$$\chi^R_{nm}(q;P):=f(-q_+^2)\chi_{nm}(q;P)f(-q_-^2), \tag{46}$$

then Eq.(43) is rewritten as

$$\begin{aligned}&S_F^{R-1}(q_+)\chi^R(q;P_B)S_F^{R-1}(q_-)\\ &\quad=\ -iC_F\int_k\frac{1}{f(-k_+^2)f(-k_-^2)}\bar{g}^2(q_E^2,k_E^2)iD^{\mu\nu}(q-k)\gamma_\mu\chi^R(k;P_B)\gamma_\nu.\end{aligned} \tag{47}$$

We see again that the integral equation is regularized correctly.

The BS amplitude for the pseudoscalar meson can be written in terms of four scalar amplitudes,

$$\begin{aligned}\chi^R_{nm}(k;P)=\delta_{ji}\frac{(\lambda^\alpha)_{gf}}{2}\Big[\Big(&\phi_S(k;P)+\phi_P(k;P)\not{k}+\phi_Q(k;P)\not{P}\\&+\frac{1}{2}\phi_T(k;P)(\not{P}\not{k}-\not{k}\not{P})\Big)\gamma_5\Big]_{ba}\end{aligned} \tag{48}$$

where λ^α denotes the flavor matrix. Substituting this into Eq.(47), we obtain coupled integral equations for four scalar amplitudes. The explicit form is rather complicated and given in appendix. The integral equations can be written down formally

$$\phi_{\mathcal{A}}(q;P_B) = \int_k \mathcal{M}_{\mathcal{AB}}(q,k;P_B)\phi_{\mathcal{B}}(k;P_B) \tag{49}$$

where $\mathcal{A},\mathcal{B}$ denotes S,P,Q,T. Among the four dimensional integration d^4k, two of the integrations can be performed analytically after the Wick rotation and we set the total momentum $P_{BE} = (M_E,0,0,0)$. Then we obtain

$$\phi_{\mathcal{A}}(q_R,q_\theta;M_E) = \int_{(k_R,k_\theta)\in I} dk_R dk_\theta \mathcal{M}_{\mathcal{AB}}(q_R,q_\theta;k_R,k_\theta;M_E)\phi_{\mathcal{B}}(k_R,k_\theta;M_E) \tag{50}$$

where

$$k_E^2 = k_R^2, \quad k_E P_E = k_R M_E \sin k_\theta \tag{51}$$

and the integral region is given by

$$I := \left\{ (k_R,k_\theta) \,\middle|\, k_R^2 \pm k_R M_E \sin k_\theta + \frac{M_E^2}{4} \le \Lambda_{\rm UV}^2 \right\}. \tag{52}$$

This integral region is determined uniquely by the cut-off function in Eq.(47) and is consistent with the SD equation (25).

There is no solution of Eq.(50) for a real M_E because M_E is a Euclidean meson mass whose square is negative $M_E^2 = -M_B^2$. Since the SD equation can be solved only for space like region $q_E^2 \ge 0$, the region $M_E^2 < 0$ is not accessible. Instead of solving Eq.(50), we convert it into an eigenvalue equation for a fixed $M_E^2 \ge 0$, given by

$$\lambda\phi_{\mathcal{A}}(q_R,q_\theta;M_E) = \int dk_R dk_\theta \mathcal{M}_{\mathcal{AB}}(q_R,q_\theta;k_R,k_\theta;M_E)\phi_{\mathcal{B}}(k_R,k_\theta;M_E) \tag{53}$$

where λ is the eigenvalue that is equal to unity for the solutions of Eq.(50). We solve Eq.(53) numerically using the iteration procedure. When we iterate Eq.(53), the eigen-function associated with the maximum absolute eigenvalue is dominated. Then we obtain the maximum eigenvalue and its eigen-function.

In the numerical calculations, we use the discretization of the continuous variable (q_R,q_θ) and come across a problem that the kernel $K_{\mathcal{AB}}$ diverges at the point $(q_R,q_\theta) = (k_R,k_\theta)$. This divergence, which is originated from the gluon propagator, does not cause a real divergence.

We may remove this divergence by carefully choosing the discretization points in the iteration procedure.

Once we obtain (the largest absolute) λ as a function of $M_E^2 \geq 0$, then we extrapolate $\lambda(M_E^2)$ to the time-like region $M_E^2 < 0$ and look for the on-shell point where $\lambda(-M_B^2) = 1$. Since this extrapolation is the most ambiguous procedure in our calculation, we will later consider another function which is similarly extrapolated to the one-shell value and compare the predicted values M_B^2 obtained in the two independent extrapolations.

6 Decay Constant and low-energy relation

To obtain the decay constant, we need the normalization of the BS amplitude. The normalization condition of the BS amplitude is derived from the inhomogeneous BS equation

$$\frac{1}{i}\frac{\delta^2\Gamma[S_F]}{\delta S_{Fmn}(x,y)\delta S_{Fn'm'}(y',x')}G^{(2)}_{C;n'm'm''n''}(y'x';x''y'') = \delta_{m''m}\delta_{nn''}\delta(x''-x)\delta(y-y'') \tag{54}$$

where

$$\begin{aligned} G^{(2)}_{C;nmm'n'}(yx;x'y') &:= \langle 0|T\psi_n(y)\overline{\psi}_m(x)\psi_{m'}(x')\overline{\psi}_{n'}(y')|0\rangle \\ &\quad - \langle 0|T\psi_n(y)\overline{\psi}_m(x)|0\rangle\langle 0|T\psi_{m'}(x')\overline{\psi}_{n'}(y')|0\rangle. \end{aligned} \tag{55}$$

In the momentum space, Eq.(54) gives

$$\begin{aligned} & i\int_q \frac{1}{f(-q_+^2)f(-q_-^2)}\chi^R_{n_1m_1}(q;P_B)\overline{\chi}^R_{m_2n_2}(q;P_B)\frac{\partial}{\partial P^\mu}\Big(S^{R-1}_{Fn_2n_1}(q_+)S^{R-1}_{Fm_1m_2}(q_-)\Big) \\ & \quad + i\int_q \frac{-(q_+)_\mu f'(-q_+^2)f(-q_-^2) - (q_-)_\mu f'(-q_-^2)f(-q_+^2)}{f^2(-q_+^2)f^2(-q_-^2)} \\ & \quad \times \chi^R_{n_1m_1}(q;P_B)S^{R-1}_{Fm_1m_2}(q_-)\overline{\chi}^R_{m_2n_2}(q;P_B)S^{R-1}_{Fn_2n_1}(q_+) = -2P_\mu, \quad P \to P_B. \end{aligned} \tag{56}$$

In the case of the sharp cut-off function (3), the second term in the LHS of Eq.(56) does not contribute and the integral region in the first term is determined uniquely.

Let us now turn to the discussion of the axial-vector Ward–Takahashi (WT) identity. It has been found that the axial-vector WT identity is violated in the Higashijima-Miransky (HM) approximation [14]. Of course the Goldstone theorem holds in this case because the HM approximation respects the global chiral symmetry. The chiral WT identity in the ladder approximation has been carefully studied in [10]. The reason of the violation of the axial-vector

WT identity is that the HM approximation breaks local chiral symmetry. As shown in [10], the improved ladder approximation of the SD and BS equations preserves the WT identity for the axial-vector vertex if and only if one uses the gluon momentum square as the argument of the running coupling constant. However, in this case renormalization factor Z_2 of the quark wave function deviates from unity in the Landau gauge. In order to avoid such problems, authors of [10] have introduced the non-local gauge so that the gauge parameter in the gluon propagator becomes a momentum dependent function. On the other hand, we have proposed another way to recover the axial-vector WT identity [15]. In this approach the axial-vector current is modified so as to become the correct Noether current of the effective model of QCD. The advantage of this approach is that it is applicable to all the effective models of QCD which respect the global chiral symmetry. According to [15], the meson decay constant can be expressed as follows*.

$$f_B = \lim_{P\to P_B}\frac{1}{P^2}\int_q \mathrm{tr}\Big[\overline{\chi}^R(q;P_B)\Big\{i\gamma_5\frac{\lambda^\alpha}{2}\Big(\frac{f(-q_-^2)+f(-q_+^2)}{2}\not{P}+(f(-q_+^2)-f(-q_-^2))\not{q}\Big) + E^\alpha(q;P)\Big\}\Big], \tag{57}$$

$$\begin{aligned} E^\alpha_{mn}(q;P) := \int_k \Big[& \Big\{\mathcal{K}^{n'n,mm'}\Big(-k,q-\frac{P}{2};-q-\frac{P}{2},k+P\Big) \\ & - \mathcal{K}^{n'n,mm'}\Big(-k,q-\frac{P}{2};-q+\frac{P}{2},k\Big)\Big\}\Big(i\gamma_5\frac{\lambda^\alpha}{2}S_F(k)\Big)_{m'n'} \\ & + \Big\{\mathcal{K}^{n'n,mm'}\Big(-k+P,q-\frac{P}{2};-q-\frac{P}{2},k\Big) \\ & - \mathcal{K}^{n'n,mm'}\Big(-k,q+\frac{P}{2};-q-\frac{P}{2},k\Big)\Big\}\Big(S_F(k)i\gamma_5\frac{\lambda^\alpha}{2}\Big)_{m'n'}\Big] \end{aligned} \tag{58}$$

The on-shell value $f_B(M_E^2=-M_B^2)$ is obtained again by extrapolation from the space like region $M_E^2>0$ to the on-shell point $M_E^2=-M_B^2$. For the neutral pion ($B=\pi^0$), $\alpha=3$ and so on in Eq.(57).

As shown in Ref.[15], the WT identity for the axial-vector vertex leads to the following relation in the improved ladder approximation model of QCD:

$$M_B^2 f_B = -2m_R(\mu^2)\mathcal{E}_B(\mu^2) \tag{59}$$

* f_π in this paper corresponds to $\tilde{f}_\pi$ in [15].

with

$$\mathcal{E}_B(\mu^2) := Z_m^{-1}(\mu^2) i \int_q \frac{f(-q_-^2) + f(-q_+^2)}{2} \mathrm{tr}\left[\overline{\chi}^R(q; P_B)\gamma_5 \frac{\lambda^\alpha}{2}\right]. \tag{60}$$

This relation is satisfied for a finite quark mass. In the case of chiral limit, we obtain

$$f_B \mathcal{E}_B(\mu^2) = \xi_R(\mu^2) \quad \text{where} \quad \xi_R := \langle \overline{\psi}\psi \rangle_R. \tag{61}$$

One can treat Eq.(61) as an approximated relation of the leading term of the expansion of m_R for finite quark mass. Substituting Eq.(61) to Eq.(59), one obtains the Gell-Mann–Oakes–Renner (GMOR) mass formula

$$M_B^2 f_B^2 \simeq -2 m_R \langle \overline{\psi}\psi \rangle_R|_{\text{chiral limit}}. \tag{62}$$

For finite $m_R > 0$, Eq.(59) is an exact relation, while the violation of the GMOR formula is incurred by the violation of Eq.(61).

We define $\mathcal{R}$ by

$$\mathcal{R}(M_E^2) := \frac{-M_E^2 f_B(M_E^2)}{-2 m_R \mathcal{E}_B}. \tag{63}$$

A relation $\mathcal{R}(-M_B^2) = 1$ must be satisfied due to Eq.(59). We use this condition to make the extrapolation more reliable.

7 Numerical results

7.1 Parameters of the model

The parameters of the improved ladder model of QCD are the current quark mass m_R for up and down quarks (The isospin symmetry is assumed throughout this paper.), the scale parameter of QCD Λ_{QCD}, the infrared cut-off t_{IF} for the running coupling constant, the smoothness parameter t_0 and the ultraviolet cut-off Λ_{UV}. We take $t_0 = -3$ throughout this paper, which is the same value used in Ref.[4]. In Ref.[4] they have shown that the numerical results are quite insensitive to the choice of the smoothness parameter in their studies of the BS amplitudes in the chiral limit. As for the ultraviolet cut-off Λ_{UV}, we shall show that the physical observables depends on it rather weakly after our renormalization procedure described in section 4, if we use reasonably

large value of $\Lambda_{\rm UV}$. Of course, as we are treating not the full QCD but its approximation, we expect that weak dependences remain in our numerical studies. Thus we only have three physically relevant parameters, namely, the current quark mass, $\Lambda_{\rm QCD}$ and the infrared cut-off.

We choose $\Lambda_{\rm QCD}$ about 0.6 [GeV]. It is rather large compared with the value obtained from the analyses in the deep inelastic scattering. In the framework of this model, however, one must employ the large value of $\Lambda_{\rm QCD}$ in order to bring sufficiently strong dynamical chiral symmetry breaking. It may be the indication of the limitation of the improved ladder approach. Other non-perturbative interactions between quarks may solve this discrepancy. One candidate for such non-perturbative interactions is the instanton induced interaction proposed by 't Hooft [16]. There have been many studies of the roles of the instanton in low-energy QCD such as the instanton liquid model [17], the generalized Nambu-Jona-Lasinio (NJL) model [18] with 't Hooft instanton induced interaction [19], the effects of the instanton in baryon sector [20]. The recent studies of the η-meson properties in the generalized NJL model with the 't Hooft instanton induced interaction have shown [21] that the contribution from the 't Hooft instanton induced interaction to the dynamical mass of the up and down quark mass is 44% of that from the usual $U_L(3) \times U_R(3)$ invariant four-quark interaction. The introduction of the 't Hooft instanton induced interaction to the ILA model seems to be interesting and such attempt is now in progress [22].

We employ $t_{\rm IF}$ about -0.5 due to Ref.[4]. The running coupling constant for various $\Lambda_{\rm QCD}$ and $t_{\rm IF}$ is shown in Figs.1 and 2.

7.2 SD equation

We discuss the solutions of the SD equation in this subsection. $B(-q_E^2)$ as solutions of Eq.(25) for various values of m_R are shown in Fig.3. In the chiral limit, i.e. $m_R = 0$, we find a non-trivial solution $B(-q_E^2)$ which is non-zero for $q_E \leq 1$GeV. Note that Eq.(25) has also a trivial solution $B(-q_E^2) = 0$, if $m_R = 0$. The existence of the non-trivial solution indicates that chiral symmetry is broken dynamically. $B(-q_E^2)$ decreases quickly to zero for $q_E \geq 1$GeV. The asymptotic behavior is consistent with the OPE result as shown in Ref.[2]. The range of non-zero value of $B(-q_E^2)$ is determined by the q_E^2 dependence of the coupling constant, $g(q_E^2)$ defined in Eq.(7). The results shown in Fig.3 correspond to the choice $\Lambda_{\rm QCD} = 0.6$ GeV. When

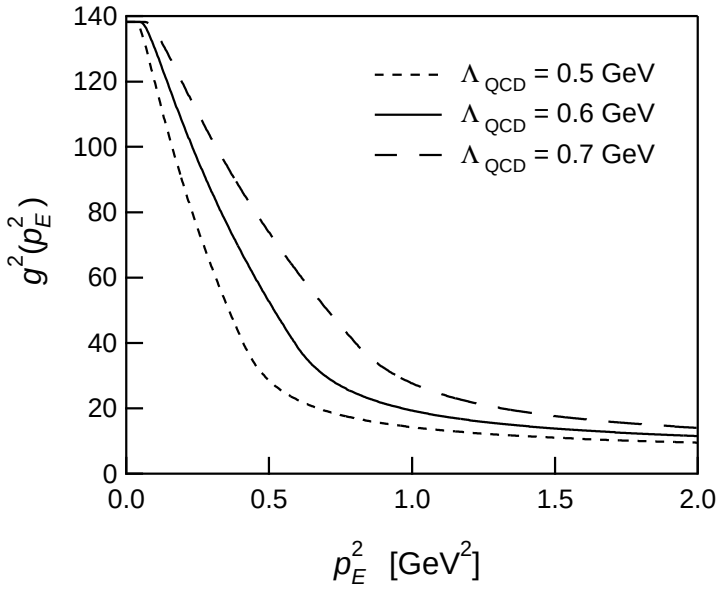

Figure 1: q_E^2 dependence of $g^2(q_E^2)$ for various $\Lambda_{\rm QCD}$ with $t_{\rm IF} = -0.5$.

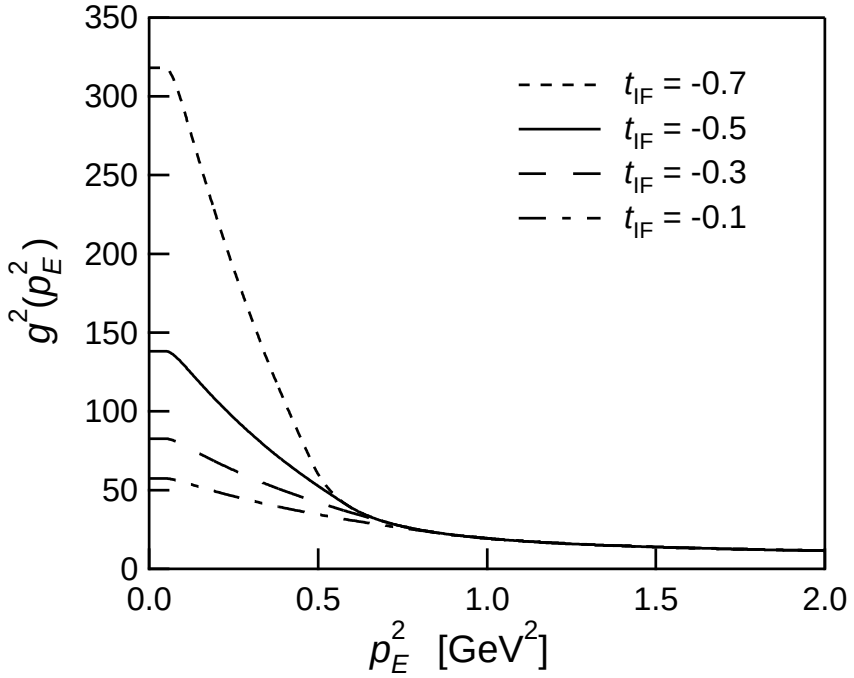

Figure 2: q_E^2 dependence of $g^2(q_E^2)$ for various t_{IF} with $\Lambda_{\rm QCD} = 0.6$GeV.

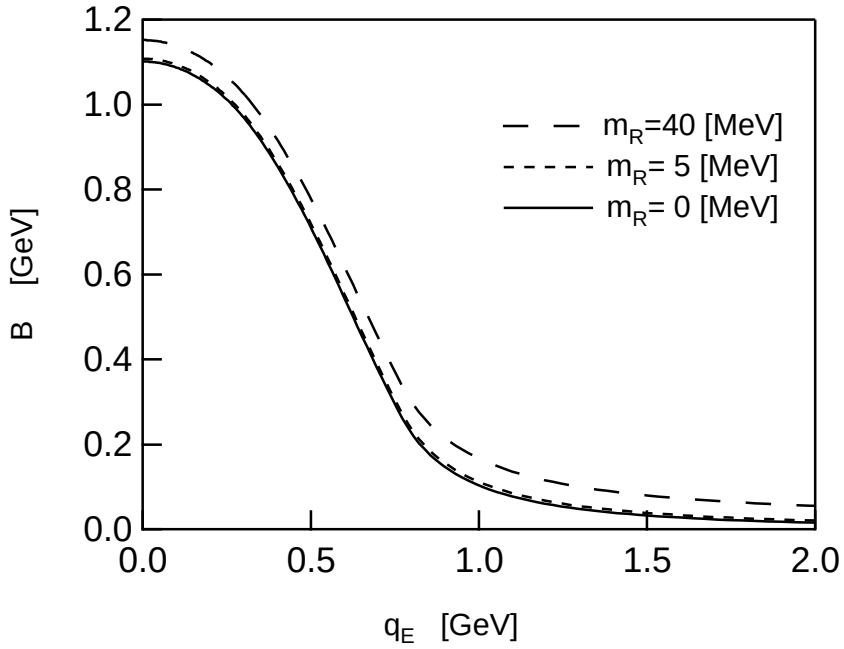

Figure 3: Quark mass function $B(-q_E^2)$ as function of q_E. Model parameters are $\Lambda_{\rm UV} = 100$ GeV, $\Lambda_{\rm QCD} = 0.6$ GeV, $t_{\rm IF} = -0.5$ and $\mu^2 = 4$ GeV^2.

$t_{\rm IF}$	-0.5	0.0	0.5	1.0	1.5	2.0
$-\langle\overline{\psi}\psi\rangle_R^{1/3}$ [MeV]	259	240	187	116	43	2

Table 1: $t_{\rm IF}$ dependence of quark condensate in the chiral limit. Other model parameters are $\Lambda_{\rm UV} = 100$ GeV, $\Lambda_{\rm QCD} = 0.6$ GeV and $\mu^2 = 4$ GeV^2.

$\Lambda_{\rm QCD}$ decreases, the range of $B(-q_E^2)$ decreases accordingly and therefore the chiral symmetry breaking is weakened. But the $\Lambda_{\rm QCD}$ determines the scale of the system. The order parameter $\langle\overline{\psi}\psi\rangle$ is almost proportional to the $\Lambda_{\rm QCD}^3$ and the chiral symmetry breaking always occurs for smaller $\Lambda_{\rm QCD}$. The parameter $t_{\rm IF}$ determines the strength of the coupling constant. Table 1 shows $t_{\rm IF}$ dependence of the condensate in the chiral limit. As can be seen from table 1, the chiral symmetry breaking does not occur for larger $t_{\rm IF}$. The asymptotic behavior of $B(-q_E^2)$ with the finite current quark mass is rather different from that in the chiral limit. It can be seen clearly from the log-log plot of the quark mass function $B(-q_E^2)$ given in Fig. 4.

We next discuss the quark condensate. The quark condensates $-\langle\overline{\psi}\psi\rangle_R^{1/3}$ calculated for the

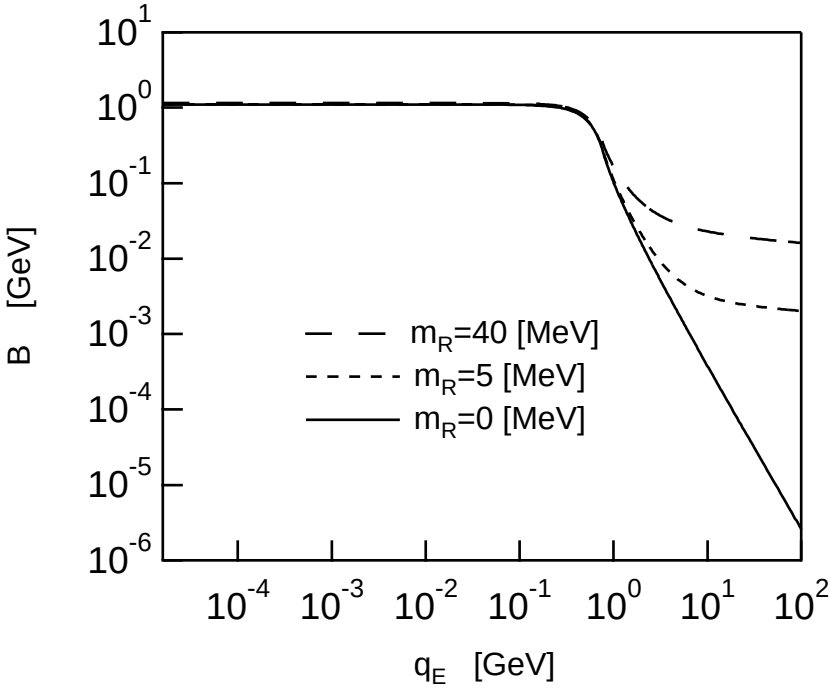

Figure 4: Log-log plot of quark mass function $B(-q_E^2)$. Model parameters are $\Lambda_{\rm UV} = 100$ GeV, $\Lambda_{\rm QCD} = 0.6$ GeV, $t_{\rm IF} = -0.5$ and $\mu^2 = 4$ GeV^2.

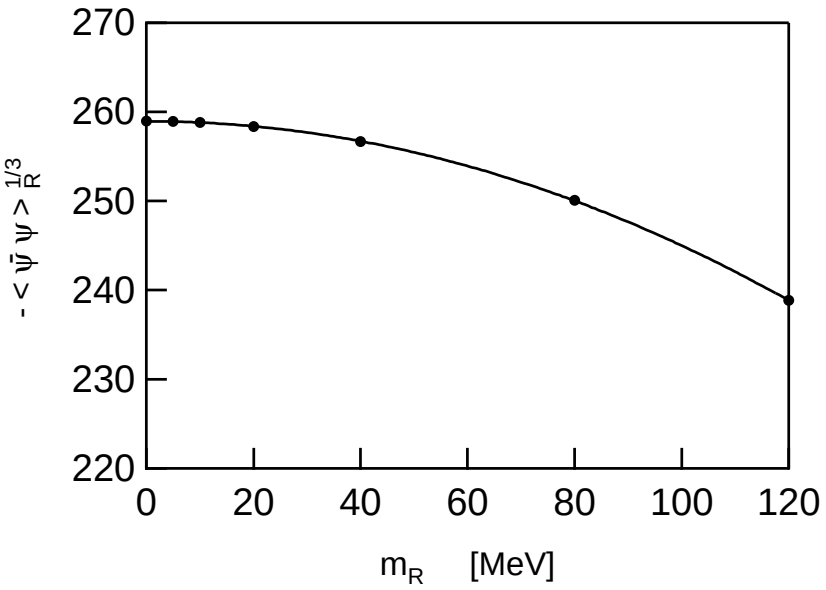

Figure 5: m_R dependence of $-\langle\overline{\psi}\psi\rangle_R^{1/3}$. Model parameters are $\Lambda_{\rm UV} = 100$ GeV, $\Lambda_{\rm QCD} = 0.6$ GeV, $t_{\rm IF} = -0.5$ and $\mu^2 = 4$ GeV^2.

various quark masses are shown in Fig. 5. Since in our definition of the quark condensate given in Eqs.(36)-(39) the perturbative quark mass contribution is subtracted, $-\langle\overline{\psi}\psi\rangle_R^{1/3}$ decreases as m_R increases. Similar behavior is observed in the QCD sum rule approach. $\langle\overline{\psi}\psi\rangle_R$ for $m_R = 120$ MeV is about 78% of $\langle\overline{\psi}\psi\rangle_R$ for $m_R = 5$ MeV. This is in reasonable agreement with the QCD sum rule result [23]: $\langle\bar{s}s\rangle/\langle\bar{u}u\rangle = 0.8 \pm 0.1$.

7.3 BS equation

Let us now turn to the discussion of the solutions of the BS equation. The eigenvalues $\lambda(M_E^2)$ of the BS equation are shown in Fig.6. One sees that the massless solution $\lambda(M_E^2 = 0) = 1$ appears in the chiral limit. This is a result of the Nambu–Goldstone theorem. For a non-zero quark mass, we need to extrapolate $\lambda(M_E^2)$ to the time-like $M_E^2 < 0$. We have fitted $\lambda(M_E^2)$ by a quadratic function using the method of least-squares and extrapolated $\lambda(M_E^2)$ to the time-like region to find the point at which $\lambda(M_E^2)$ becomes unity. Fig.6 implies that the extrapolation length is longer for larger quark mass. In order to reduce the ambiguity in the extrapolation procedure, we also evaluate the ratio $\mathcal{R}$ defined by Eq.(63) as a function of M_E^2. Because of the

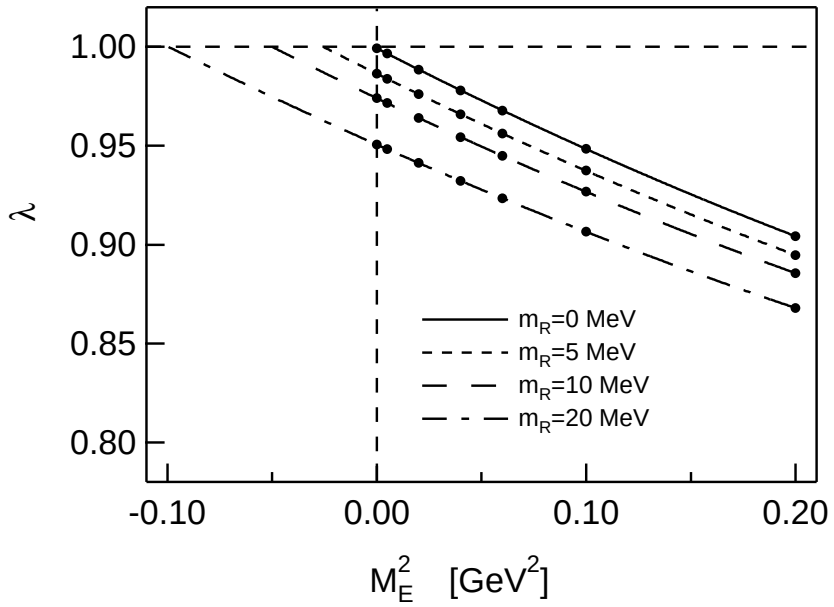

Figure 6: Eigenvalues of BS equation $\lambda(M_E^2)$. Model parameters are $\Lambda_{\rm UV} = 100$ GeV, $\Lambda_{\rm QCD} = 0.6$ GeV, $t_{\rm IF} = -0.5$ and $\mu^2 = 4$ GeV^2.

exact relation (59), $\mathcal{R}$ must hit $\mathcal{R}(-M_\pi^2) = 1$ at the on-mass-shell of the pion. The value $\mathcal{R}$ is shown in Fig.7. We fit the graph with the linear function using the methods of least-squares. We show our calculated results of the pion mass M_π determined by the above mentioned two conditions, i.e., $\lambda = 1$ and $\mathcal{R} = 1$, for various values of the quark mass m_R in table 2. The ambiguity by the extrapolation procedure is reasonably small up to the strange quark mass region. We plot our results of M_π^2 obtained by the condition $\lambda = 1$ as a function of m_R in Fig. 8. The M_π^2 seems to be almost a linear function of m_R up to $m_R \sim 40$ MeV. This is suggested

m_R	0	5	10	20	40	80	120
M_π $(\lambda = 1)$	0.0	159.1	222.0	312.9	444.4	639.8	800.9
M_π $(\mathcal{R} = 1)$	0.0	154.5	218.5	309.0	436.9	616.1	749.7

Table 2: Pion masses determined by the two conditions, $\lambda = 1$ and $\mathcal{R} = 1$ for various values of m_R. All the entries are in units of MeV. Model parameters are $\Lambda_{\rm UV} = 100$ GeV, $\Lambda_{\rm QCD} = 0.6$ GeV, $t_{\rm IF} = -0.5$ and $\mu^2 = 4$ GeV^2.

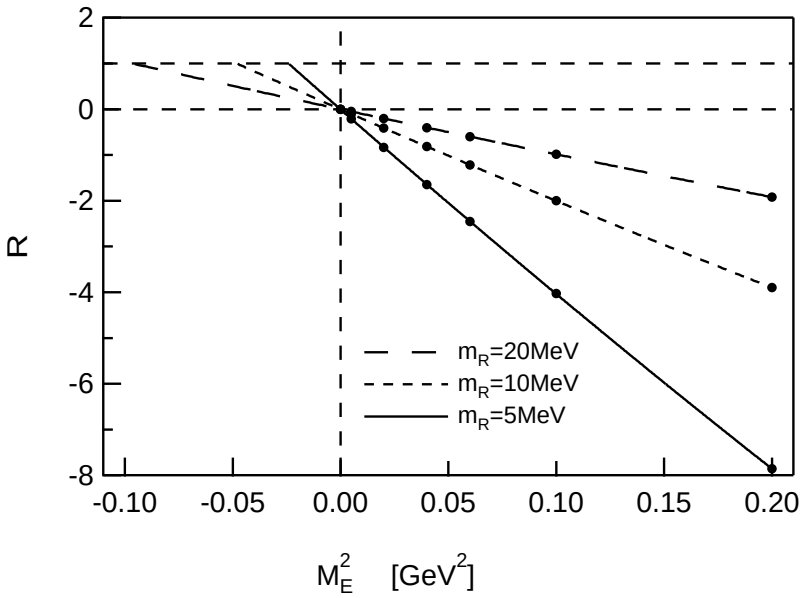

Figure 7: The value $\mathcal{R}(M_E^2)$. Model parameters are $\Lambda_{\rm UV} = 100$ GeV, $\Lambda_{\rm QCD} = 0.6$ GeV, $t_{\rm IF} = -0.5$ and $\mu^2 = 4$ GeV^2.

by the GMOR formula

$$M_\pi^2 \simeq \left(\frac{-2\langle \overline{\psi}\psi \rangle_R}{f_\pi^2} \right)_{\text{chiral limit}} m_R \,. \tag{64}$$

The deviation from the linear dependence at $m_R = 120$ MeV is about 9%.

We next discuss the pion decay constant. As mentioned in Sec. 6, we can calculate $f_\pi(M_E^2)$ only for the time-like M_E^2 and therefore the on-shell value of the decay constant $f_\pi(M_E^2 = -M_\pi^2)$ can be obtained again by the extrapolation. The M_E^2 dependence of the pion decay constants in the chiral limit and in the case of $m_R = 5$ MeV are shown in Fig. 9.

To estimate the effect of $E^\alpha(q;P)$ in Eq.(57), we plot the naive value f_π^N which is defined by neglecting $E^\alpha(q;P)$ term from Eq.(57). It seems to be a good approximation that $f_\pi(M_E^2)$ is a linear function of M_E^2. Therefore we fit the curve by the linear function using the method of least-squares and make an extrapolation to the time-like M_E^2 for finite m [*]. On the other hand, we fit f_π^N by the quadratic function using the least-square method to extrapolate to the

[*] It should be noted that the decay constant at small (positive) M_E^2 suffers from numerical uncertainty and thus it deviates from the straight line. We do not use these points in our extrapolation procedure.

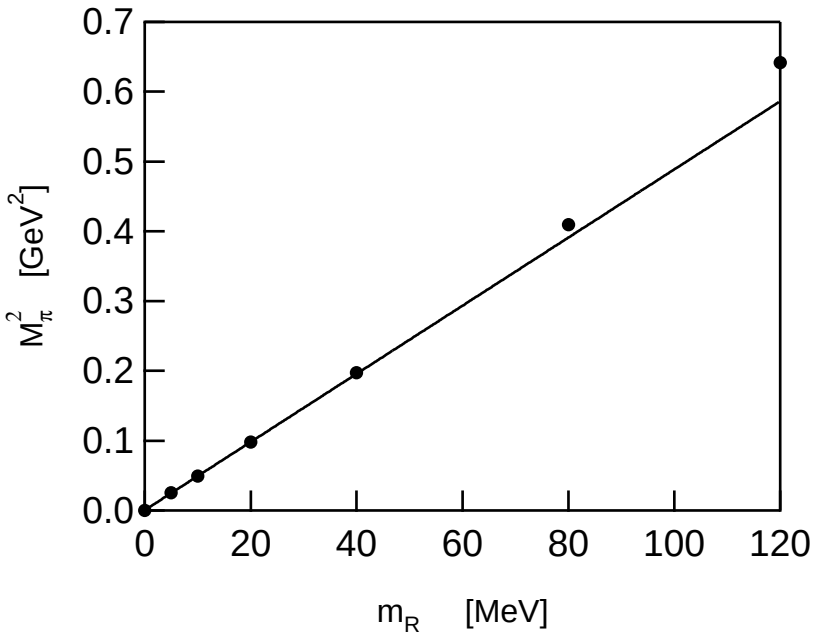

Figure 8: M_π^2 as a function of m_R. Dots represent our calculated results and line represents the linear fit of the first 4 points. Model parameters are $\Lambda_{\rm UV} = 100$ GeV, $\Lambda_{\rm QCD} = 0.6$ GeV, $t_{\rm IF} = -0.5$ and $\mu^2 = 4$ GeV^2.

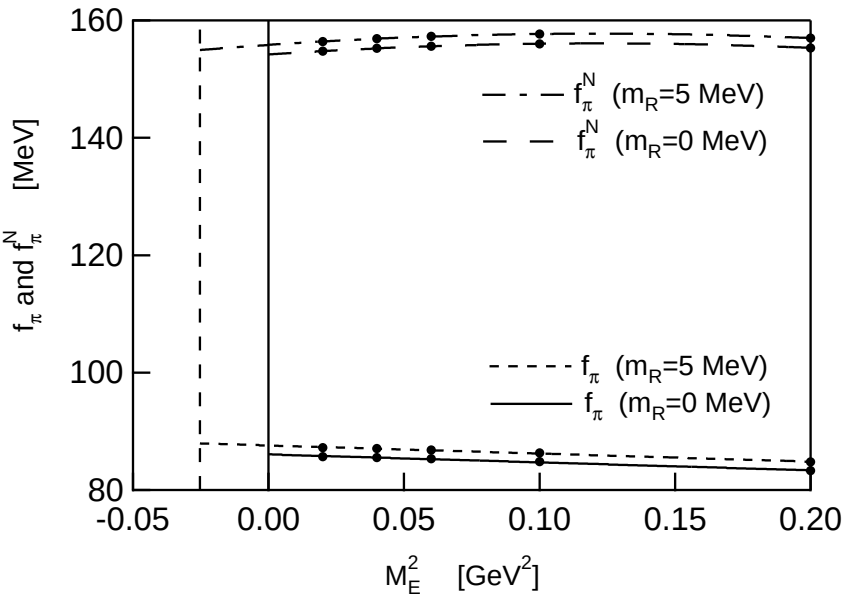

Figure 9: M_E^2 dependence of f_π and f_π^N. Vertical dashed line represents the point $M_E^2 = -M_\pi^2$ for $m_R = 5$ MeV. Model parameters are $\Lambda_{\rm UV} = 100$ GeV, $\Lambda_{\rm QCD} = 0.6$ GeV, $t_{\rm IF} = -0.5$ and $\mu^2 = 4$ GeV^2.

on-shell point $M_E^2 = M_\pi^2$. Our results for $m_R = 5$ MeV are $f_\pi = 88$ MeV and $f_\pi^N = 155$ MeV, so the contribution of $E^\alpha(q;P)$ term is remarkable. Similar result has been found in the ILA model which respects the axial-vector WT identity by using the gluon momentum square as the argument of the running coupling constant and the non-local gauge [10]. The condition $\mathcal{R}(-M_\pi^2) = 1$ is the direct consequence of the axial-vector WT identity and therefore it has been proved numerically that our definition of the decay constant is consistent with the axial-vector WT identity from the fact that the pion mass determined by the condition $\lambda = 1$ is almost same as that determined by the condition $\mathcal{R} = 1$.

We plot the quark mass dependence of the decay constant in Fig. 10. f_π almost linearly depends on m_R in our case. f_π at $m_R = 40$ MeV is about 15% bigger than f_π at $m_R = 5$ MeV and f_π at $m_R = 80$ MeV is about 32% bigger than f_π at $m_R = 5$ MeV. Since the observed $f_K/f_\pi = 1.23$, m_R dependence of the decay constant seems to be reasonable though we have not solved the kaon BS equation. This m_R dependence of f_π is similar to that obtained in the chiral perturbation theory (ChPT) [24] though the chiral log term has not been seen in our numerical result. It is understandable because the Goldstone boson loop contribution is

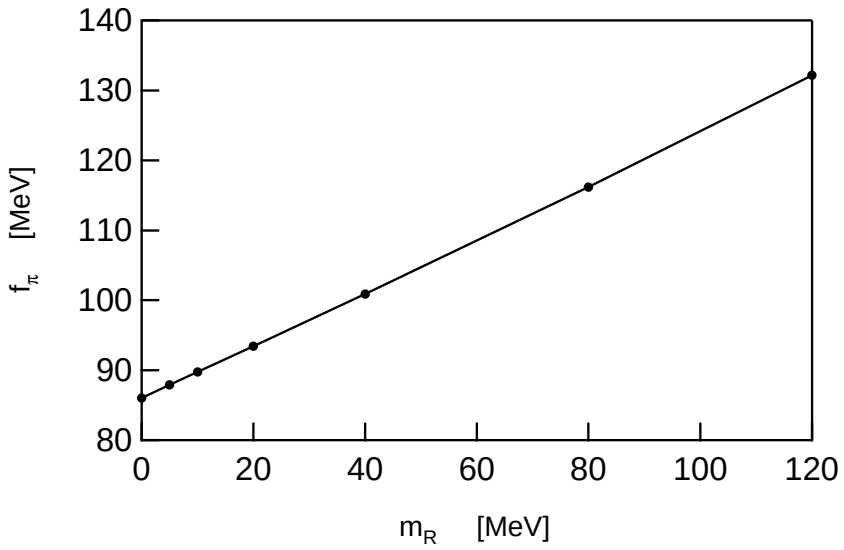

Figure 10: m_R dependence of f_π. Model parameters are $\Lambda_{\rm UV} = 100$ GeV, $\Lambda_{\rm QCD} = 0.6$ GeV, $t_{\rm IF} = -0.5$ and $\mu^2 = 4$ GeV^2.

$\Lambda_{\rm QCD}$ [GeV]	M_π [MeV]	f_π [MeV]	$-\langle\overline{\psi}\psi\rangle_R^{1/3}$ [MeV]
0.5	152	74	223
0.6	159	88	259
0.7	166	102	293

Table 3: $\Lambda_{\rm QCD}$ dependences of M_π, f_π and $-\langle\overline{\psi}\psi\rangle_R^{1/3}$. Other model parameters are $\Lambda_{\rm UV} = 100$ GeV, $t_{\rm IF} = -0.5$, $\mu^2 = 4$ GeV^2 and $m_R = 5$ MeV.

not taken into account explicitly in our approach. On the other hand, the quark-antiquark structure is included explicitly and the finite quark mass effects are fully taken into account without performing the perturbative expansion with respect to the quark mass.

Let us now discuss the $\Lambda_{\rm QCD}$ and the $t_{\rm IF}$ dependences. Table 3 shows the $\Lambda_{\rm QCD}$ dependences of the pion mass, the pion decay constant and the quark condensate. As shown in Table 3, the all the quantities with the mass dimension one are roughly proportional to the $\Lambda_{\rm QCD}$. It is understandable since the only scale of the theory is the $\Lambda_{\rm QCD}$ if one can neglect the current quark mass. Table 4 shows the $t_{\rm IF}$ dependence. For $t_{\rm IF}$ below -0.7 the coupling constant

$t_{\rm IF}$	M_π [MeV]	f_π [MeV]	$-\langle\overline{\psi}\psi\rangle_R^{1/3}$ [MeV]
-0.3	149	91	256
-0.5	159	88	259
-0.7	(181)	(74)	(253)

Table 4: $t_{\rm IF}$ dependences of M_π, f_π and $-\langle\overline{\psi}\psi\rangle_R^{1/3}$. Other model parameters are $\Lambda_{\rm UV} = 100$ GeV, $\Lambda_{\rm QCD} = 0.6$ GeV, $\mu^2 = 4$ GeV^2 and $m_R = 5$ MeV.

becomes very steep and our numerical procedure is not sufficiently accurate. Although we have not performed the fine tuning of the model parameters, it is clear from Tables 1, 3 and 4 that one can fit the model parameters so as to reproduce the observed values of M_π and f_π and the empirically determined value of the quark condensate.

We study the $\Lambda_{\rm UV}$ dependence by changing the value of $\Lambda_{\rm UV}$ from 10 GeV to 1000 GeV. It causes less than 1% changes of the M_π, f_π and $\langle\overline{\psi}\psi\rangle_R$. This stability indicates that our non-perturbative renormalization procedure works well.

7.4 Approximation

Finally we discuss the approximation often used in solving the BS equation. The approximation in which one neglects the ϕ_P, ϕ_Q, ϕ_T terms in RHS in the BS equation (49) is often used in literatures [25]. The resulting eigenvalues are shown in Fig.11. While this approximation gives the massless NG boson in the chiral limit, it underestimates the pion mass for finite quark mass. The decay constants obtained from the approximated BS amplitude are shown in Table 5. The approximation overestimates the pion decay constant about 30% while the axial-vector WT identity $(M_\pi^{\rm Appro.})^2 f_\pi^{\rm Appro.} = -2m_R\mathcal{E}_\pi^{\rm Appro.}$ is preserved. It is seen that the effect of $E^\alpha(q;P)$ is very small in this case, and $f_\pi^{\rm Appro.} \simeq f_\pi^{N\rm Appro.}$. Therefore, the violation of the axial-vector WT identity or that of the exact relation for the PCAC current incured by neglecting $E^\alpha(q;P)$ effect is very small.

The above $f_\pi^{\rm Appro.}$ is calculated in a similar way as in the approximation discussed in Ref.[15, 26]. The following is shown in theorem 2 of [26]. If the interaction is local chiral invariant,

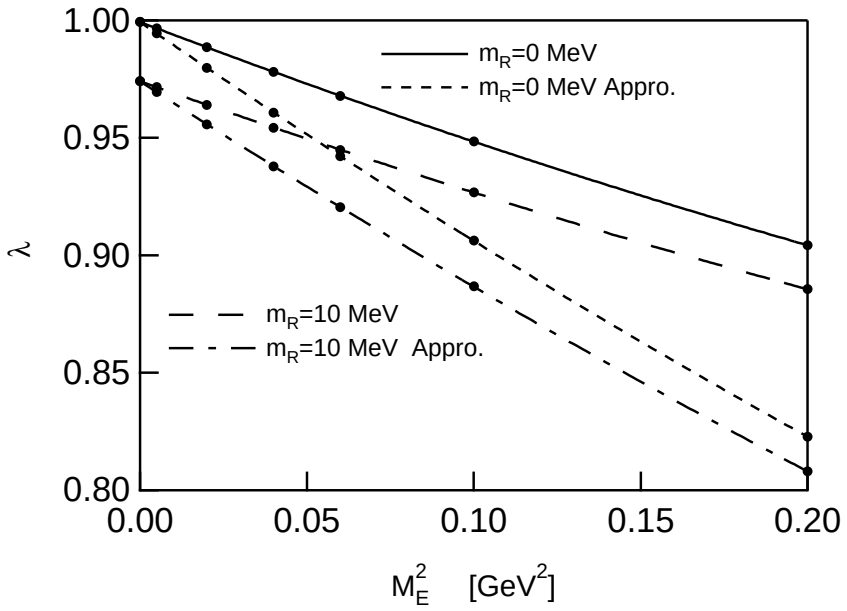

Figure 11: Eigenvalues of the BS equations with and without the approximation described in the text. Model parameters are $\Lambda_{\rm UV} = 100$ GeV, $\Lambda_{\rm QCD} = 0.6$ GeV, $t_{\rm IF} = -0.5$ and $\mu^2 = 4$ GeV^2.

m_R	M_π	$M_\pi^{\rm Appro.}$	f_π	$f_\pi^{\rm Appro.}$	f_π^N	$f_\pi^{N\rm Appro.}$
0	0	0	86	115	154	116
5	159	119	88	117	156	117
10	222	166	90	118	158	119

Table 5: Result with and without Approximation. All the entries are in units of MeV. Model parameters are $\Lambda_{\rm UV} = 100$ GeV, $\Lambda_{\rm QCD} = 0.6$ GeV, $t_{\rm IF} = -0.5$ and $\mu^2 = 4$ GeV^2.

the approximation of taking the wave function renormalization of the quark propagator to be one and at the same time neglecting the ϕ_P, ϕ_Q and ϕ_T terms in the RHS of the BS equation preserves the low-energy relations. This theorem cannot be applied to the present case since the interaction term of the ILA model breaks the local chiral symmetry. However one can prove that the low-energy relation holds if one neglects the ϕ_P and ϕ_Q terms in $E^\alpha(q;P)$ as well as the ϕ_P, ϕ_Q and ϕ_T terms in the RHS of the BS equation by following the same argument of the proof of theorem 2 in [26].

8 Conclusion

We have solved the Schwinger–Dyson (SD) equation for the quark propagator and the Bethe–Salpeter (BS) equation for the pion in the improved ladder approximation of QCD. We have carefully treated the consistency of the equations in order to preserve the low-energy relations associated with chiral symmetry by using the Cornwall–Jackiw–Tomboulis effective action approach. We have introduced the finite quark mass term in order to study effects of explicit chiral symmetry breaking on the low-energy relations. Because of the difference in the asymptotic behavior of the quark mass function for finite quark mass, the non-perturbative mass-independent renormalization has been introduced and the quark condensate for finite quark mass is calculated. In solving the SD and BS equations, we have not taken any further approximation such as expansion of BS amplitudes in the Gegenbauer polynomials.

We have obtained reasonable values of M_π, f_π and $\langle\overline{\psi}\psi\rangle_R$ with a rather large value of $\Lambda_{\rm QCD}$. It may indicate the limitation of the improved ladder approach. The pion mass M_π grows as quark mass m_R increases. Up to the strange quark mass region M_π^2 seems to be proportional to quark mass m_R almost as predicted by the GMOR relation

$$M_\pi^2 = \left(\frac{-2\langle\overline{\psi}\psi\rangle_R}{f_\pi^2}\right)_{\text{chiral limit}} m_R. \tag{65}$$

We have found that the f_π also grows as m_R increases almost linearly. The m_R dependences of M_π^2 and f_π are similar to those obtained in the chiral perturbation theory. It suggests that the chiral perturbation is applicable up to the strange quark mass region.

We have studied the effect of $E^\alpha(q;P)$ term in the true decay constant. We have found that it is significantly large for various input parameters. Therefore in the framework of the

improved ladder approximation, $E^\alpha(q;P)$ plays an essential role to keep the chiral property.

We have further shown the result of the approximation neglecting $\phi_P(q;P), \phi_Q(q;P)$ and $\phi_T(q;P)$ term in RHS of the BS equations. This approximation is very useful and makes the calculation easy greatly. But the result gives a smaller pion mass. This suggests that the simple picture of the $\phi_S(q;P)$ dominance in the BS equation is not so good, at least in the present model.

So far, we have studied the symmetric q-$\bar{q}$ systems, $u\bar{u}$, $d\bar{d}$, etc. It is interesting to extend the present formulation to asymmetric systems like the kaon. It is also interesting to introduce the $U_A(1)$ breaking interaction to this framework and to study the η-η' systems. Such attempts are in progress.

Acknowledgment

The authors would like to thank Kensuke Kusaka for useful discussions. This work is supported in part by the Grant-in-Aid for Scientific Research (A)(1)08304024 and (C)(2)08640356 of the Ministry of Education, Science, Sports and Culture of Japan.

Appendix

Here we write down the BS equation explicitly. In this section the total momentum is denoted by P instead by P_B for simplicity. First we define the regularized amputated BS amplitude $\hat{\chi}^R(q;P)$ by

$$\hat{\chi}^R(q;P) := S_F^{R-1}(q+\frac{P}{2})\chi^R(q;P)S_F^{R-1}(q-\frac{P}{2}), \tag{66}$$

which can be expressed in terms of

$$\hat{\chi}^R_{nm}(q;P) = \delta_{ji}\frac{(\lambda^a)_{gf}}{2}\Big[\Big(\hat{\phi}_S(q;P) + \hat{\phi}_P(q;P)\not{q} + \hat{\phi}_Q(q;P)\not{P} + \frac{1}{2}\hat{\phi}_T(q;P)(\not{P}\not{q} - \not{q}\not{P})\Big)\gamma_5\Big]_{ba}. \tag{67}$$

The BS equation (49) reads

$$\hat{\phi}_{\mathcal{A}}(q;P) = \int_k K_{\mathcal{AB}}(q,k;P)\phi_{\mathcal{B}}(k;P). \tag{68}$$

The components of the kernel is given explicitly by

$$K_{SS}(q,k;P) = iC_F\bar{g}^2(q,k)\frac{-3}{(q-k)^2} \tag{69}$$

$$K_{PP}(q,k;P) = \frac{iC_F\bar{g}^2(q,k)}{P^2q^2-(Pq)^2}\Big\{\frac{P^2(qk)-(Pq)(Pk)}{(q-k)^2} + \frac{2(qk-k^2)(P^2q^2-(Pq)^2+(Pq)(Pk)-P^2(qk))}{(q-k)^4}\Big\} \tag{70}$$

$$K_{PQ}(q,k;P) = \frac{iC_F\bar{g}^2(q,k)}{P^2q^2-(Pq)^2}\cdot\frac{2(Pq-Pk)(P^2q^2-(Pq)^2+(Pq)(Pk)-P^2(qk))}{(q-k)^4} \tag{71}$$

$$K_{QP}(q,k;P) = \frac{iC_F\bar{g}^2(q,k)}{P^2q^2-(Pq)^2}\Big\{\frac{(Pk)q^2-(Pq)(qk)}{(q-k)^2} + \frac{2(qk-k^2)((Pq)(qk)-(Pk)q^2)}{(q-k)^4}\Big\} \tag{72}$$

$$K_{QQ}(q,k;P) = \frac{iC_F\bar{g}^2(q,k)}{P^2q^2-(Pq)^2}\Big\{\frac{P^2q^2-(Pq)^2}{(q-k)^2} + \frac{2(Pq-Pk)((Pq)(Pk)-(qk)q^2)}{(q-k)^4}\Big\} \tag{73}$$

$$K_{TT}(q,k;P) = \frac{iC_F\bar{g}^2(q,k)}{P^2q^2-(Pq)^2}\cdot\frac{1}{(q-k)^4}\Big\{(k^2-q^2)((Pq)(Pk)-P^2(qk)) + 2(Pq-Pk)((Pk)q^2-(Pq)(qk))-2(qk-k^2)(P^2q^2-(Pq)^2)\Big\} \tag{74}$$

and other components are zero. The relations between $\phi_{\mathcal{A}}(q;P)$ and $\hat{\phi}_{\mathcal{A}}(q;P)$ are given by

$$\phi_S(q;P) = \frac{1}{\Delta}\Big[\Big\{q^2-\frac{P^2}{4}-B(q_+^2)B(q_-^2)\Big\}\hat{\phi}_S(q;P) + \Big\{q^2(B(q_+^2)-B(q_-^2))-\frac{Pq}{2}(B(q_-^2)+B(q_+^2))\Big\}\hat{\phi}_P(q;P) + \Big\{(Pq)(B(q_+^2)-B(q_-^2))-\frac{P^2}{2}(B(q_-^2)+B(q_+^2))\Big\}\hat{\phi}_Q(q;P) + (P^2q^2-(Pq)^2)\hat{\phi}_T(q;P)\Big] \tag{75}$$

$$\phi_P(q;P) = \frac{1}{\Delta}\Big[(B(q_+^2)-B(q_-^2))\hat{\phi}_S(q;P) + \Big\{q^2+\frac{P^2}{4}-B(q_+^2)B(q_-^2)\Big\}\hat{\phi}_P(q;P) + 2(Pq)\hat{\phi}_Q(q;P) - \Big\{(Pq)(B(q_-^2)+B(q_+^2))+\frac{P^2}{2}(B(q_-^2)-B(q_+^2))\Big\}\hat{\phi}_T(q;P)\Big] \tag{76}$$

$$\phi_Q(q;P) = \frac{1}{\Delta}\Big[-\frac{1}{2}(B(q_+^2)+B(q_-^2))\hat{\phi}_S(q;P)$$

$$
\begin{aligned}
& - \frac{Pq}{2}\hat{\phi}_P(q;P) \\
& - \left\{ q^2 + \frac{P^2}{4} + B(q_+^2)B(q_-^2) \right\} \hat{\phi}_Q(q;P) \\
& + \left\{ q^2(B(q_-^2) + B(q_+^2)) + \frac{Pq}{2}(B(q_-^2) - B(q_+^2)) \right\} \hat{\phi}_T(q;P) \Bigg] \qquad (77)
\end{aligned}
$$

$$
\begin{aligned}
\phi_T(q;P) \;=\; & \frac{1}{\Delta}\Bigg[\hat{\phi}_S(q;P) - \frac{1}{2}(B(q_-^2) - B(q_+^2))\hat{\phi}_P(q;P) \\
& + (B(q_+^2) + B(q_-^2))\hat{\phi}_q(q;P) \\
& + \left\{ -q^2 + \frac{P^2}{4} - B(q_-^2)B(q_+^2) \right\} \hat{\phi}_T(q;P) \Bigg] \qquad (78)
\end{aligned}
$$

where

$$
\Delta := (q_+^2 - B^2(q_+^2))(q_-^2 - B^2(q_-^2)). \qquad (79)
$$

References

[1] J.M. Cornwall, R. Jackiw and E. Tomboulis, Phys. Rev. **D10** (1974) 2428.

[2] K. Higashijima, Phys. Rev. **D29** (1984) 1228.

[3] V.A. Miransky, Sov. J.Nucl. Phys. **38** (1984) 280.

[4] K. Aoki, M. Bando, T. Kugo, M. G. Mitchard and H. Nakatani, Prog. Theor. Phys. **84**(1990) 683

[5] K.-I. Aoki, M. Bando, T. Kugo and M. Mitchard, Prog. Theor. Phys. **85** (1991) 355.

[6] K.-I. Aoki, T. Kugo and M. Mitchard, Phys. Lett. **B266** (1991) 467.

[7] For a review, C. D. Roberts and A. G. Williams, Prog. Part. Nucl. Phys. **33** (1994) 477.

[8] For a recent study, P. Maris and C. D. Roberts, Phys. Rev. **C56** (1997) 3369, and references therein.

[9] K.-I. Aoki, "Non-perturbative Renormalization Group Approach to Dynamical Chiral Symmetry Breaking in Gauge Theories", Proceedings of the International Workshop on

Perspectives of Strong Coupling Gauge Theories, Edited by J. Nishimura and K. Yamawaki, World Scientific 1997, p171.

[10] T. Kugo and M. Mitchard, Phys. Lett. **B282** (1992) 162.

[11] K. Kusaka, H. Toki and S. Umisedo, in preparation.

[12] C. D. Roberts and A. G. Williams, Prog. Part. Nucl. Phys. **33** (1994) 477

[13] H.D. Politzer, Nucl. Phys. **B117** (1976) 397.

[14] P. Jain and H.J. Munczek, Phys. Rev. **D44** (1991) 1873.

[15] K. Naito, K. Yoshida, Y. Nemoto, M. Oka and M. Takizawa, "*Dynamical Chiral Symmetry Breaking in Effective Models of QCD in the Bethe–Salpeter Approach*", hep-ph/9805243.

[16] G. 't Hooft, Phys. Rev. **D14** (1976) 3432.

[17] E.V. Shuryak, Nucl. Phys. **B203** (1982) 93; **B203** (1982) 116; D.I. Diakonov and V.Yu. Petrov, Nucl. Phys. **B272** (1986) 457; M.A. Nowak, J.J.M. Verbaarschot and I. Zahed, Nucl. Phys. **B324** (1989) 1; T. Schäfer and E.V. Shuryak, Phys. Rev. **D53** (1996) 6522; **D54** (1996) 1099; Rev. Mod. Phys. **70** (1998) 323.

[18] Y. Nambu and G. Jona-Lasinio, Phys. Rev. **122** (1961) 345; **124** (1961) 246.

[19] T. Kunihiro and T. Hatsuda, Phys. Lett. **B206** (1988) 385; T. Hatsuda and T. Kunihiro, Z. Phys. **C51** (1991) 49; Phys. Rep. **247** (1994) 221; V. Bernard, R.L. Jaffe and U.-G. Meissner, Nucl. Phys. **B308** (1988) 753; Y. Kohyama, K. Kubodera and M. Takizawa, Phys. Lett. **B208** (1988) 165; M. Takizawa, K. Tsushima, Y. Kohyama and K. Kubodera, Prog. Theor. Phys. **82** (1989) 481; Nucl. Phys. **A507** (1990) 611; H. Reinhardt and R. Alkofer, Phys. Lett. **B207** (1988) 482; R. Alkofer and H. Reinhardt, Z. Phys. **C45** (1989) 275; S. Klimt, M. Lutz, U. Vogl and W. Weise, Nucl. Phys. **A516** (1990) 429; U. Vogl, M. Lutz, S. Klimt and W. Weise, Prog. Part. Nucl. Phys. **27** (1991) 195.

[20] E.V. Shuryak and J.L. Rosner, Phys. Lett. **B218** (1989) 72; M. Oka and S. Takeuchi, Phys. Rev. Lett. **63** (1989) 1780; Nucl. Phys. **A524** (1991) 649; S. Takeuchi and M. Oka, Phys.

Rev. Lett. **66** (1991) 1271; O. Morimatsu and M. Takizawa, Nucl. Phys. **A554** (1993) 635; S. Takeuchi, Phys. Rev. Lett. **73** (1994) 2173; Phys. Rev. **D53** (1996) 6619.

[21] M. Takizawa and M. Oka, Phys. Lett. **B359** (1995) 210; **B364** (1995) 249 (E); Y.Nemoto, M. Oka and M. Takizawa, Phys. Rev. **D54** (1996) 6777; M. Takizawa, Y.Nemoto and M. Oka, Phys. Rev. **D55** (1997) 4083.

[22] K. Naito, K. Yoshida, Y. Nemoto, M. Oka and M. Takizawa in preparation.

[23] L.J. Reinders, H. Rubinstein and S. Yazaki, Phys. Rep. **127** (1985) 1.

[24] J. Gasser and H. Leutwyler, Ann. Phys. (N.Y.) **158** (1984) 142; Nucl. Phys. **B250** (1985) 465.

[25] M. R. Frank and C. D. Roberts, Phys. Rev. **C53** (1996) 390; C. Savkli and F. Tabakin, Nucl. Phys. **A628** (1998) 645.

[26] K. Naito and M. Oka, "*Approximation of the Schwinger–Dyson and the Bethe–Salpeter Equations and Chiral Symmetry of QCD*", hep-ph/9805258, to appear in Phys. Rev. C.